

Determining the workspace boundary of 6-DOF parallel manipulators

K. Y. Tsai*, T. K. Lee* and K. D. Huang†

(Received in Final Form: December 18, 2005. First published online: February 28, 2006)

SUMMARY

The workspace boundary of 6-DOF parallel manipulators is a two-dimensional surface consisting of many patches that can be obtained by solving different sets of four constraint equations. This paper proposes algorithms for finding the equations to generate each patch of the boundary. Methods involving a searching technique are first developed to generate some small subsets of the boundary. The obtained data are then used to predict the equations for generating the rest of the boundary.

KEYWORDS: Reachable workspace; 6-DOF parallel manipulator; Link interaction.

I. INTRODUCTION

The workspace of a manipulator has been studied by many researchers over the past three decades. Currently, the research interests are focused on the workspace of parallel manipulators. This paper investigates the reachable workspace of 6-DOF Stewart-Gough parallel manipulators.

The reachable workspace can be determined by a discretization method.¹ A point is in the workspace if the point can be approached by at least one orientation of the platform. However, many boundary points can be reached by only one orientation. To find the exact orientation for these boundary points is a very time-consuming task. A geometric approach is a more reliable method for developing the exact boundary of the workspace. Haug *et al.* developed algorithms for mapping boundaries of manipulator workspaces.^{2,3} For the 6-DOF Stewart platform, singular curves in the z -level cutting plane are obtained by solving 20 equations (in 21 variables) developed from the kinematic constraints (related to limited actuator's strokes) and the row rank deficiency of a matrix. Barrier analysis is then performed to determine the boundary of the workspace.

The admissible solutions (real solutions that do not violate any kinematic constraint) of all possible sets of four constraint equations generate many two-dimensional singular surfaces. The intersections of these singular surfaces

are many one-dimensional curves called bifurcation curves. Bifurcation curves divide the singular surfaces into many two-dimensional patches. The boundary of workspace consists of some outmost external patches that the reference point on the platform cannot penetrate. This paper presents the rules for determining the equations to generate each patch of the boundary. Algorithms based on these rules are then proposed to develop the boundary of workspace.

II. CONSTRAINT EQUATIONS

Figure 1 shows a spatial 6-DOF, 6SPS parallel manipulator. Two coordinate frames A (X, Y, Z) and B (u, v, w) are attached to the fixed base and moving platform, respectively. The attachment points A_i for $i = 1$ to 6 are on the fixed base, and attachment points B_i for $i = 1$ to 6 are on the platform. The constraint equations for developing the boundary surface can be found in the literature.^{4–6} In general, the equations can be expressed as

$$f_i(x, y, z, \alpha, \beta, \gamma) = q_i \quad (1)$$

where x, y, z, α, β and γ denote the six parameters that specify the position and orientation of the platform, and q_i represents limb length ρ_i , the angle (denoted by ϕ_i) between the straight line associated to limb i and the axes of symmetry of a spherical joint, or the distance between limbs i and j (denoted by d_{ij}). Let Q_i and Q_j be the intersecting points of the common perpendicular of limbs i and j with the two limbs respectively. If all six limbs are approximated by cylinders with a diameter D , then limbs i and j interfere if Q_i is on limb i , Q_j is on limb j , and $d_{ij} \leq D$. The equations with q_i at limited positions are used as the constraint equations for developing boundary patches. We assume that the combinations of four constraints from Eq. (1) and possible kinematic singularities of a manipulator do not generate boundary patches. In theory, it is possible that these combinations can generate boundary patches for some very special designs. In this case, the effects of kinematic singularities cannot be neglected.

In this paper, the boundary of workspace is represented by the consecutive intersecting curves of the boundary surface and the vertical planes through the z -axis of the reference frame. A vertical plane (denoted by ZX^+) is a half-plane spanned by the positive x' -axis and the z' -axis of frame A' (X', Y', Z') obtained by the rotation matrix about the z -axis of the fixed frame. A typical intersecting boundary curve on a ZX^+ plane is shown in Fig. 2, where P_i for $i = 1$ to $(n - 1)$ denote bifurcation points. For most symmetric manipulators,

* Department of Mechanical Engineering, National Taiwan University of Science and Technology, 43 Keelung Road, Section 4, Taipei (Taiwan) 10672.

E-mail: kytsai@mail.ntust.edu.tw

† Department of Mechanical Engineering, Northern Taiwan Institute of Science and Technology, Taipei (Taiwan).

Corresponding author: K. Y. Tsai; E-mail: kytsai@mail.ntust.edu.tw

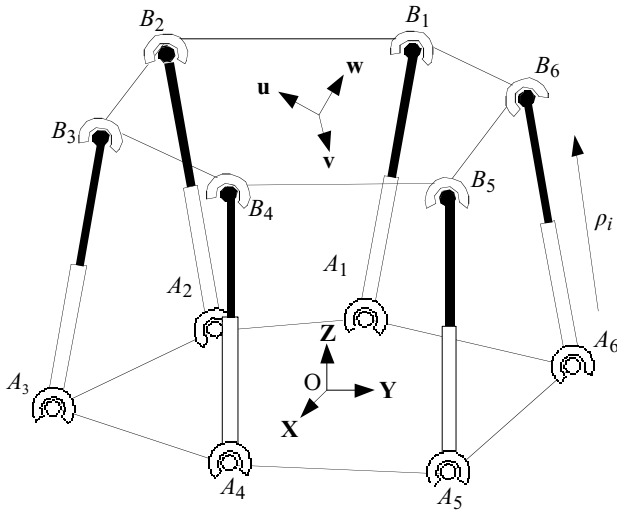


Fig. 1. A 6-DOF parallel manipulator.

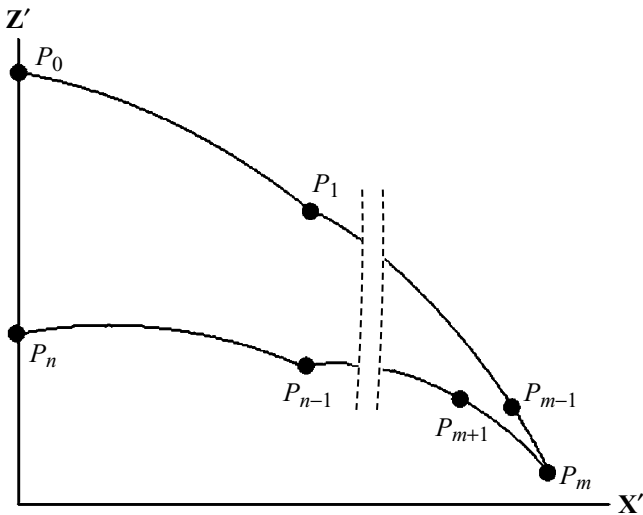


Fig. 2. A cross-section of workspace.

P₀ and P_n are extreme points with $\rho_{j\max} = \rho_j$ and $\rho_{j\min} = \rho_j$ (for $j = 1$ to 6), respectively. The segments between points P₀ and P_m (the point of maximum reach in the x'-direction) and the segments between points P_m and P_n are termed upper and lower boundary curves respectively. The segments (generated by different sets of four constraint equations) on these curves are connected by bifurcation or extreme points. Any point on the boundary obtained by any existing method can be used as the initial point to develop boundary. Starting from the initial point, we let $y=0$, $x = x + \Delta x$ (with A' as the reference frame) and solve the four corresponding constraint equations to compute the next boundary point. The solution of z, α, β, γ can be easily obtained if the current values of z, α, β and γ are used as the initial values. If the solution does not converge at some isolated singular points, then we change Δx to avoid singularities. The process is repeated until the path reaches a bifurcation point or an extreme point. At bifurcation or extreme points, there are many possible combinations of constraint equations to generate the next segment, so we need an efficient method for determining the correct combination to generate the next segment on the boundary curve.

Taking the time derivatives of Eq. (1), we have

$$\nabla f_i \cdot \mathbf{T} = \dot{q}_i \tag{2}$$

with $\mathbf{T} = [\dot{\alpha} \ \dot{\beta} \ \dot{\gamma} \ \dot{x} \ \dot{y} \ \dot{z}]^t$

where $\dot{q}_i = 0$ if $\rho_{i\max} = q_i$, $\rho_{i\min} = q_i$, $\phi_{i\max} = \phi_i$, or $D = d_{ij}$. Suppose that there are m constraint equations ($m \leq 6$) reaching their corresponding limited positions and their gradients are independent. Then we can develop a 6×6 matrix \mathbf{M} with the m gradients as the first m rows and the remaining $(6-m)$ rows can be the gradients of other constraint equations or any constant vectors such that \mathbf{M} is not singular. Let

$$\mathbf{H} = \mathbf{M}^{-1} \equiv \begin{bmatrix} \mathbf{e}_1 & \mathbf{e}_2 & \cdots & \mathbf{e}_6 \\ \mathbf{h}_1 & \mathbf{h}_2 & \cdots & \mathbf{h}_6 \end{bmatrix} \tag{3}$$

If $m = 4$, then the last two columns of \mathbf{H} are orthogonal to the gradients of the four constraint equations. Therefore, the two columns span the set of all possible vectors of \mathbf{T} , and vectors \mathbf{h}_5 and \mathbf{h}_6 span the plane tangent to the singular surface generated by the four constraint equations. In what follows, vectors $\mathbf{h}_1, \mathbf{h}_2, \dots, \mathbf{h}_6$ (after being transformed to frame A') are used to find the correct combination of equations for generating the next segment at a bifurcation or an extreme point.

III. BIFURCATION AND EXTREME POINTS

Five constraint equations reach limited positions at a bifurcation point, so we have to loosen one kinematic constraint in order to generate the next segment on the boundary curve. Note that the reference point on the platform is allowed to move in only one direction, positive \mathbf{h}_k or negative \mathbf{h}_k , when we loosen the k th kinematic constraint. Therefore, we must change the direction of \mathbf{h}_k (that is, let $\mathbf{h}_k = -\mathbf{h}_k$) at $\rho_{k\max} = \rho_k$, or $\phi_{k\max} = \phi_k$ because $\dot{\rho}_k$ or $\dot{\phi}_k$ cannot be positive at the limited position. Suppose that the i th kinematic constraint is released from the limited position. Then vectors $\pm \mathbf{h}_6$ and \mathbf{h}_i span a half-plane as shown in Fig. 3a. If the half-plane, denoted by HP_{i6} , intersects the ZX^+ plane, then the four remaining constraint equations may generate a one-dimensional singular curve on the ZX^+ plane with the intersection line of planes HP_{i6} and ZX^+ as its tangent vector. The tangent vector of the curve on the ZX^+ plane is given by

$$\mathbf{t}_{i6} = \begin{bmatrix} 0 \\ 1 \\ 0 \end{bmatrix} \times (\mathbf{h}_i \times \mathbf{h}_6) \tag{4}$$

Unit vector $\hat{\mathbf{e}}_i$ in Fig. 3a satisfies $\hat{\mathbf{e}}_i \cdot \mathbf{h}_6 = 0$ and $\hat{\mathbf{e}}_i \cdot \mathbf{h}_i > 0$. The singular curve is generated in forward direction (moving away from the z-axis) if $\hat{\mathbf{e}}_i(x) > 0$ or generated in backward direction if $\hat{\mathbf{e}}_i(x) < 0$. The $x, y,$ or z in parentheses following a vector denotes the $x-, y-,$ or z -component, respectively, of the vector. The steps for finding the constraint constraints to generate the next boundary segment are given below:

1. Compute \mathbf{h}_i for $i = 1, 2, \dots, 6$.
2. Develop unit vector $\hat{\mathbf{e}}_j$ for $j = 1$ to 5 .

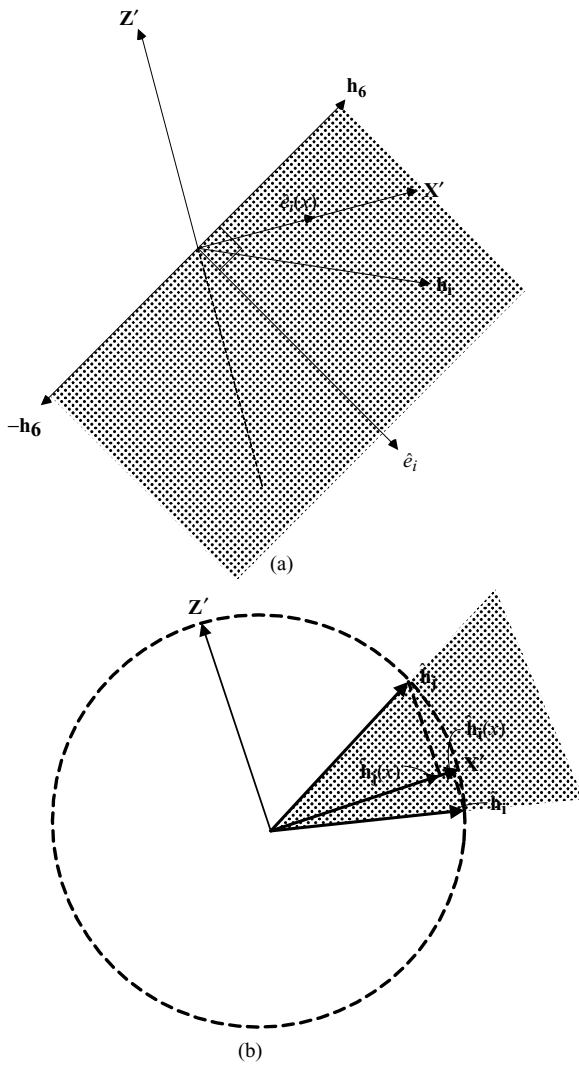


Fig. 3 Intersections of two planes.

3. (a) For forward motion, choose \mathbf{h}_j with $\hat{e}_j(x) > 0$ and compute \mathbf{t}_{j6} . Find the pair, \mathbf{h}_j and \mathbf{h}_6 , with the maximum slope, defined as $\mathbf{t}_{j6}(z)/\mathbf{t}_{j6}(x)$, for the upper boundary segments or the pair with the minimum slope for the lower boundary segments.
- (b) For backward motion, choose \mathbf{h}_j with $\hat{e}_j(x) < 0$ and compute \mathbf{t}_{j6} . Find the pair with the maximum slope for the lower boundary segments or the pair with the minimum slope for the upper boundary segments.

Except at the point of maximum reach, the remaining four equations (with j th equation excluded) will generate the next boundary segment.

Bifurcation curves intersect at some isolated extreme points where six constraint equations are at their limited positions. At an extreme point, all six rows of \mathbf{M} are generated by the gradients of the constraint equations. Therefore, we have to loosen two kinematic constraints in order to generate a curve on the ZX^+ plane, meaning that there are 15 possible combinations to choose from. Suppose that the i th and j th kinematic constraints are released from the limited positions. Then the two corresponding (unidirectional) vectors, \mathbf{h}_i and

\mathbf{h}_j , span a quarter-plane (denoted by QP_{ij}). If the quarter-plane intersects the ZX^+ plane (as illustrated in Fig. 3b), then the four remaining constraint equations may generate a one-dimensional singular curve on the ZX^+ plane with the intersection line of QP_{ij} and ZX^+ as its tangent vector. The two planes intersect if $\mathbf{h}_i(y) * \mathbf{h}_j(y) \leq 0$. Let $\hat{\mathbf{h}}_k \equiv \mathbf{h}_k / \|\mathbf{h}_k\|$. Then the moving direction, forward or backward, of the curve can be determined by the sum of the two x -components: $\hat{\mathbf{h}}_i(x)$ and $\hat{\mathbf{h}}_j(x)$. The steps for determining the equations to generate the next segment at an extreme point are given below:

1. Develop matrix \mathbf{H} and compute $\hat{\mathbf{h}}_k$ for $k = 1, 2, \dots, 6$.
2. Find all possible pairs of $\hat{\mathbf{h}}_i$ and $\hat{\mathbf{h}}_j$ satisfying $\hat{\mathbf{h}}_i(y) * \hat{\mathbf{h}}_j(y) \leq 0$ and $\hat{\mathbf{h}}_i(x) + \hat{\mathbf{h}}_j(x) > 0$ for forward motion (or $\hat{\mathbf{h}}_i(x) + \hat{\mathbf{h}}_j(x) < 0$ for backward motion).
3. If two or more pairs of $\hat{\mathbf{h}}_i$ and $\hat{\mathbf{h}}_j$ are obtained in Step 2, then find the pair with maximum slope for forward motion on the upper boundary segments (or for backward motion on the lower boundary segments), or find the pair with minimum slope for backward motion on the upper boundary segments (or for forward motion on the lower boundary segments).

With i th and j th equations removed from the set of six equations, the remaining four equations will generate the next segment.

IV. ALGORITHMS

IV.1. Algorithm for developing a boundary curve

Starting from the initial point, we develop the boundary in forward direction until x cannot be increased. The maximum point reached, in general, is a bifurcation point or an extreme point. In this case, we can find the new constraint equations to generate boundary segments in backward direction. The process is repeated until the curve returns to the z -axis. If the maximum point reached is a general boundary point with infinite slope, then we let $z = z - \Delta z$ (or $z = z + \Delta z$ if the initial point is on a lower boundary segment) and solve for x to make the path go backward in the correct direction. The path is then moved backward until the curve returns to the z -axis. Next, we develop the rest of the boundary (from the initial point to the z -axis in backward direction) to obtain a closed boundary curve.

Algorithm (I)

1. Obtain a boundary point and use it as the initial point. (If necessary, barrier analysis of singular surfaces² can be employed to check if a correct boundary point is obtained).
2. Repeat letting $x = x + \Delta x$ and solving for z, α, β, γ until a bifurcation point or an extreme point is reached, or the path can not go forward. Go to Step 4 if the path cannot go forward.
3. Employ the rules at a bifurcation or an extreme point to obtain the constraint equations for developing the next segment. Go to Step 2.
4. Go to Step 7 if the maximum point reached is not a bifurcation or an extreme point. Employ the rules at

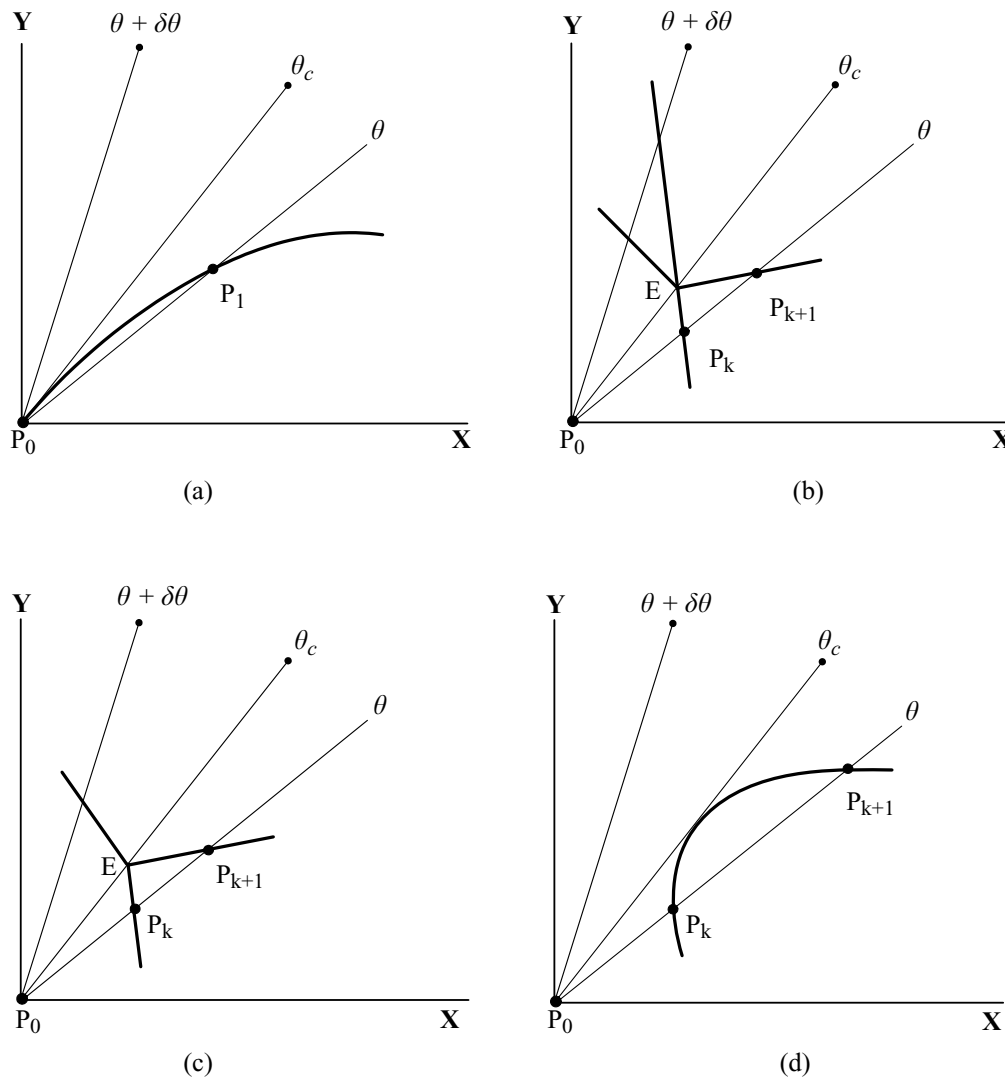


Fig. 4. Different types of boundary segments.

a bifurcation or extreme point to find the constraint equations for going backward.

5. Repeat letting $x = x - \Delta x$ and solving for z, α, β, γ until a bifurcation point or an extreme point is reached, or the path returns to the z -axis. Go to Step 8 if the path returns to the z -axis.
6. Employ the rules at a bifurcation or an extreme point to obtain the constraint equations for developing the next segment. Go to Step 5.
7. Let $z = z - \Delta z$ (or $z = z + \Delta z$ if the initial point is on the lower boundary) and solve for x, α, β, γ . Go to Step 5.
8. Develop the rest of the boundary following a similar procedure. Exit.

IV.2. Algorithm for developing boundary surface

The x - and y -coordinates (with respect to the fixed reference frame) of a point on the ZX^+ plane at θ satisfy $y = x \tan \theta$. The equation and the five equations that generate a bifurcation point on the current ZX^+ plane at θ can be used to obtain a corresponding bifurcation point on the next ZX^+ plane at $\theta + \delta \theta$. The solution $(x, y, z, \alpha, \beta, \gamma)$ can be easily obtained using a numerical technique with the current values as the

initial values. The equations, however, may yield inadmissible solutions: complex solutions or real solutions that violate some kinematic constraints. Let $P'_1, P'_2, \dots, P'_{n-1}$ denote the corresponding bifurcation points of the boundary at $\theta + \delta \theta$. Then some possible changes of boundary segments and their relations with the solutions of $P'_1, P'_2, \dots, P'_{n-1}$ are discussed below:

1. Figure 4a shows that a bifurcation curve emanates from extreme point P_0 (with $\rho_{i\max} = \rho_i$ for $i = 1, 2, \dots, 6$) at angle θ_c between θ and $\theta + \delta \theta$. If the boundaries are developed from θ to $\theta + \delta \theta$, then bifurcation point P_1 gradually approaches extreme point P_0 , and segment P_0P_1 vanishes when the solution of P'_1 turns inadmissible. Segment P_0P_1 is denoted as a Type 1 segment, which has one bifurcation point and one extreme point at the two ends.
2. Bifurcation points P_k and P_{k+1} in Fig. 4b or 4c are on two different bifurcation curves. The two curves intersect at extreme point E . When $\theta > \theta_c$, the bifurcation points (and the segment between them) corresponding to the inadmissible solutions vanish, and new bifurcation

points and segments may emerge at $\theta + \delta\theta$. The segment between the two bifurcation points (generated by different sets of constraint equations) is denoted as a Type 2 segment.

3. The bifurcation curve in Fig. 4d intersects twice the ZX⁺ plane. The bifurcation points and the segment (called a Type 3 segment in this work) between them will vanish when the solutions of P'_k and P'_{k+1} become inadmissible.

If the boundary curves are developed from $\theta + \delta\theta$ to θ , then the emergence of Type 1 or Type 3 segments cannot be detected by the solutions of $P'_1, P'_2, \dots, P'_{n-1}$. Therefore, we cannot develop the boundaries simply by solving for the bifurcation points. In this paper, we first develop the boundaries of two sections at θ_a and $\theta_b = \theta_a + \Delta\theta$. In this case, whether any Type 1 or Type 3 segment emerges at the opposite section can be detected. The related data of the two boundaries are then used to facilitate the process of developing the boundaries between the two sections.

If any new Type 1 or Type 3 segment emerges in one of the two sections, then it is easier to develop the boundaries from the section to the other. The extra segments will vanish somewhere between θ_a and θ_b . On the other hand, if the boundaries are developed in the opposite direction, then we have to determine where new Type 1 or Type 3 segments emerge. Angle θ_c in Fig. 4a can be computed if we know which bifurcation curve emanates from the extreme point. Suppose that the union of the equations that generate the first segments at θ_a and θ_b does not include the *i*th constraint equation. Then we can loosen the *i*th constraint from the extreme point to find θ_c . By letting $\rho_i = \rho_{i\max} - \delta\rho_i$ and solving the forward kinematics, we can obtain parameters *x*, *y*, *z*, α , β and γ . Angle θ_c , termed critical angle in this work, can be determined by $\theta_c = a \tan 2(x,y)$. The Type 1 segments change when θ passes θ_c .

The emergence of any Type 2 segment can be detected by solving for the bifurcation points at the next section. Segment $P_k P_{k+1}$ in Fig. 4b or 4c will vanish at $\theta + \delta\theta$ if the solutions of P'_k and P'_{k+1} are inadmissible. In this case, the standard procedure (the steps used in Algorithm (I)) can be used to develop the segments from P'_{k-1} to P'_{k+2} . Let S(a) and S(b) denote the sets of Type 3 segments on the boundaries of θ_a and θ_b , respectively. Then the following algorithm can be used to obtain the boundaries between the two sections if (i) S(a) and S(b) are nil sets; (ii) S(a) = S(a) \cup S(b); or (iii) S(b) = S(a) \cup S(b). The statements in parentheses are used when the boundaries are developed from θ_b to θ_a .

Algorithm (II)

1. If two boundaries at θ_a and θ_b are generated by the same sequence of constraint equations, then the boundaries between θ_a and θ_b are developed by the same sequence of constraint equations. Exit.
2. Let Type1U = Type1L = 0. Go to Step 5 if S(a) and S(b) are nil sets.
3. If S(a) = S(a) \cup S(b), then develop the boundaries from θ_a to θ_b . Go to Step 5.
4. If S(b) = S(a) \cup S(b), then develop the boundaries from θ_b to θ_a .

5. If the Type 1 segments on the upper boundary curves at θ_a and θ_b are different, then compute the corresponding critical angle θ_c . Let Type1U = 1.
6. If the Type 1 segments on the lower boundary curves at θ_a and θ_b are different, then compute the corresponding critical angle θ'_c . Let Type1L = 1.
7. Let $\theta = \theta + \delta\theta$ (or $\theta = \theta - \delta\theta$). Exit if $\theta \geq \theta_b$ (or $\theta \leq \theta_a$).
8. Solve for $P'_1, P'_2, \dots, P'_{n-1}$.
9. Go to Step 11 if Type1U \neq 1 and Type1L \neq 1.
10. Use the equations that generate the Type 1 segment at $\theta_b(\theta_a)$ to generate the new Type 1 segment if a critical angle is reached.
11. If two solutions of P'_i and P'_{i+1} (with corresponding P_i and P_{i+1} are the two end points of a Type 3 segment at the previous section) become inadmissible, then remove the two bifurcation points along with the segment from the current sequence.
12. If the solution of P'_k or the solutions of P'_k and P'_{k+1} corresponding to a Type 2 segment become inadmissible, then develop the boundary from P'_{k-1} to P'_{k+1} or from P'_{k-1} to P'_{k+2} using the standard procedure.
13. Develop the rest of segments. The segment between two legitimate bifurcation points P'_j and P'_{j+1} is developed using the equations that generate the segment between P_j and P_{j+1} .
14. Modify the current sequence. If the current sequence is the same as the sequence that generates the boundary at $\theta_b(\theta_a)$, then develop the remaining boundaries following the current sequence. Exit.
15. Go to Step 7.

Two boundaries at θ_a and θ_b with different Type 3 segments are illustrated in Fig. 5. The case shown in Fig. 5a is easier to handle because each section between θ_a and θ_b has at most one Type 3 segment. If we take $\Delta\theta = \Delta\theta/2$ in Fig. 5b, then a Type 3 segment will vanish at θ'_b when we develop the boundaries from $\theta_d = \theta_a + \Delta\theta/2$ to θ_a , and a Type 3 segment at θ_d will vanish at θ'_a when the boundaries are developed from θ_d to θ_b . By this approach, the boundaries between θ_a to θ_d (and the boundaries between θ_d to θ_b) can be developed using the second algorithm. The steps for developing the boundaries between two sections with different Type 3 segments are as follows:

1. Develop the boundaries from θ_a to θ_b (with positive increment) until θ reaches an angle (θ'_a in Fig. 5) where all Type 3 segments vanish.
2. Develop the boundaries from θ_b to θ_a (with negative increment) until θ reaches an angle (θ'_b in Fig. 5) where all Type 3 segments vanish.
3. If $\theta'_a \leq \theta'_b$, then develop the boundaries between θ'_a and θ'_b using the second algorithm. Exit.
4. Repeat (i) let $\Delta\theta = \Delta\theta/2$ and $\theta_b = \theta_a + \Delta\theta$; (ii) develop the boundary of θ_b until two boundaries at θ_a and θ_b satisfy S(a) = S(a) \cup S(b) or S(b) = S(a) \cup S(b).
5. Use the second algorithm to develop the boundaries between θ_a and θ_b . Exit.

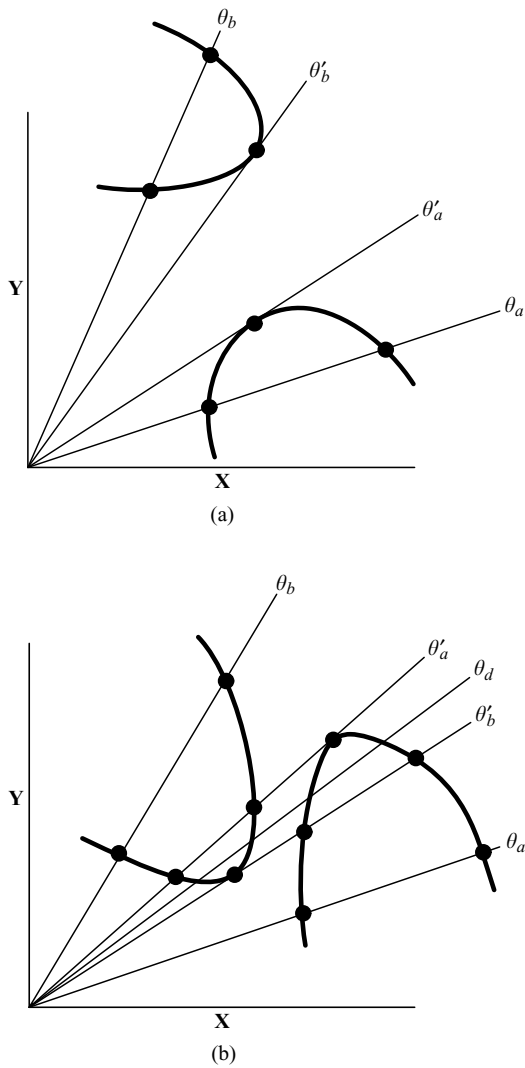


Fig. 5. Cross-sections with Type 3 segments.

The following algorithm applies these steps and the first two algorithms to develop the boundary of workspace.

Algorithm (III)

1. Let $\theta_e = 2\pi$. If the manipulator is symmetric, then $\theta_e = 2\pi/3$. Use the first algorithm to develop the boundary at $\theta_a = 0$. Record the related data.
2. Let $\theta_b = \theta_a + \Delta\theta$. Exit if $\theta_b \geq \theta_e$. Develop the boundary at θ_b . Record the related data.
3. If two boundaries at θ_a and θ_b do not have different Type 3 segments, then develop the boundaries between θ_a and θ_b using the second algorithm. Let $\theta_a = \theta_b$. Go to Step 2.
4. Develop the boundaries following the steps for the case that two sections have different Type 3 segments. Let $\theta_a = \theta_b$. Go to Step 2.

V. NUMERICAL EXAMPLE

Figure 6 shows the distribution of the spherical joints on the base and platform of a Symmetric Simplified Manipulator¹ with $55 \leq \rho_i \leq 60$ for $i = 1, 2, \dots, 6$, $\phi_{j\max} = 50^\circ$ for all the

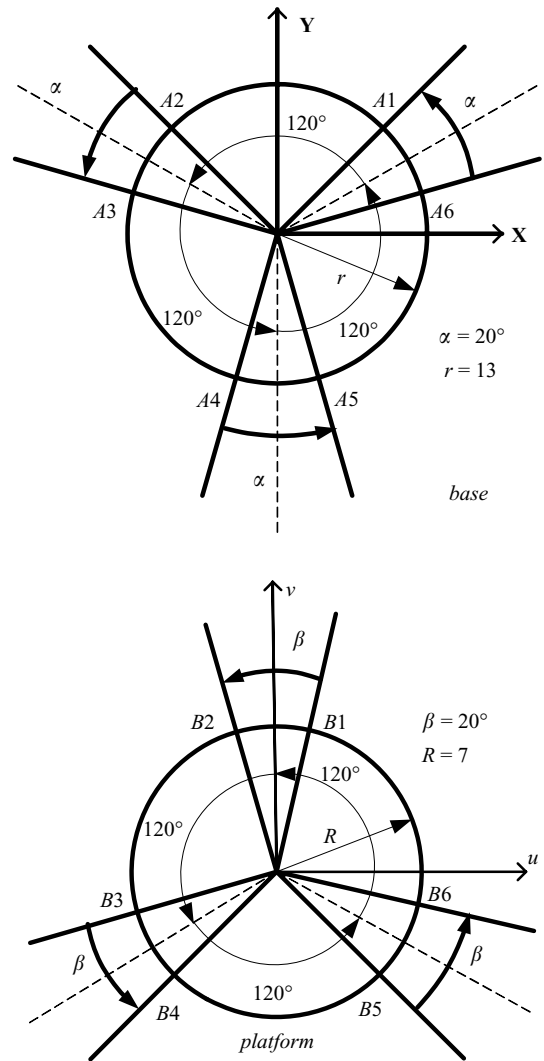


Fig. 6. The distribution of the spherical joints on the base and platform.

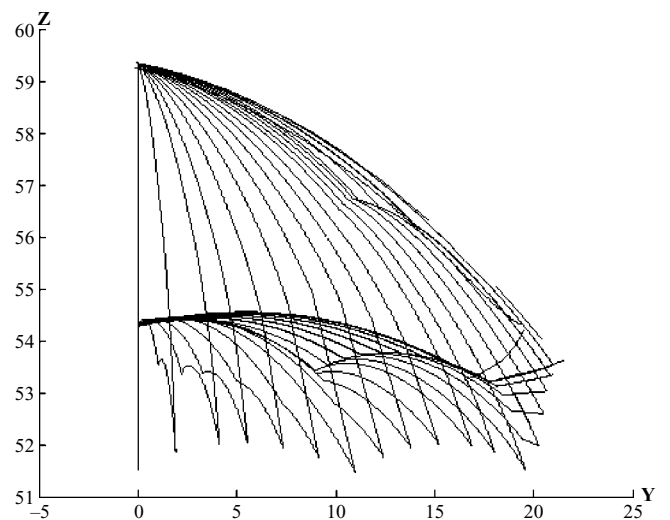


Fig. 7. Isometric view of the boundary.

spherical joints, and $D = 3$. The boundary obtained is shown in Fig. 7. No passive joint limit or link interaction is detected for the given link parameters. Next, we reduce $\phi_{j\max}$ to 25° . In this case, some passive joints reach their limited positions.

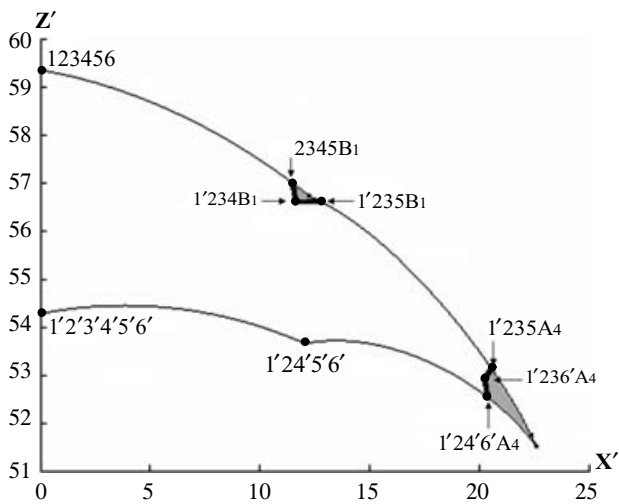


Fig. 8. The cross-section of workspace at $\theta = 0^\circ$.

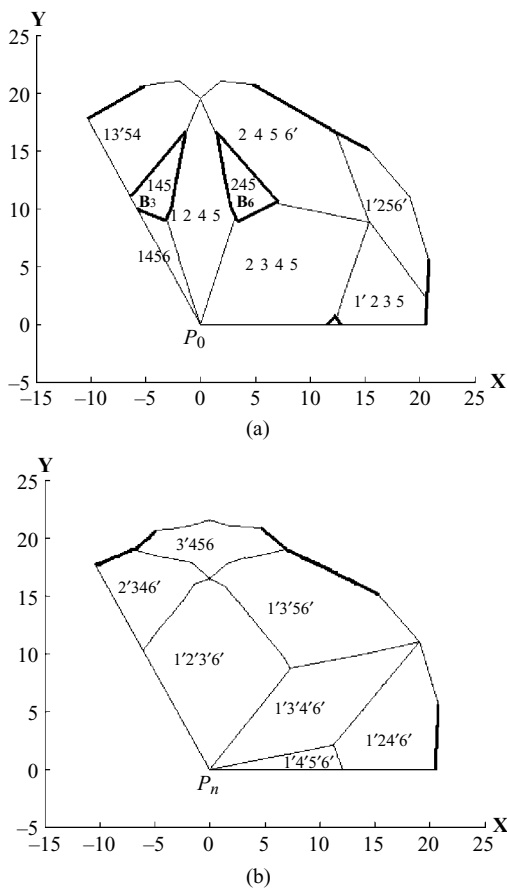


Fig. 9. The upper and lower boundary surfaces.

The cross-section of workspace at $\theta = 0^\circ$ is shown in Fig. 8 (with two shaded regions excluded from the workspace for $\phi_{jmax} = 25^\circ$), where the numbers with (') denote the

corresponding limbs are at the lower limited positions, and character A_i or B_j denotes the corresponding passive joint reaches its limit position. The top views of the upper and lower boundaries are presented in Fig. 9. It shows that the workspace can be determined by the boundary curves from $\theta = 0^\circ$ to $\pi/2$ for a symmetric manipulator.

VI. CONCLUSION

This paper presents algorithms for searching the equations that generate the workspace boundary. Some boundary curves were first obtained by searching techniques. The related data of these boundaries along with the solutions of bifurcations points of neighboring sections were then used to predict the equations for generating the rest of the boundary curves. In theory, there are hundreds of possible combinations of equations that can generate two-dimensional singular surfaces. Although the proposed algorithms obtain directly the workspace boundary, it is still a very complicated task to develop the boundary if all possible limited positions can be reached. For safety reasons, most parallel manipulators are designed in a way that they can stay away from passive joint limits, link interactions, and singular positions (by choosing proper ranges of actuator strokes). Developing the boundary of those manipulators is relatively simple because only a very small subset of the boundary is developed by searching techniques. For future workspace, the method can be extended to other types of parallel manipulators or used to design parallel manipulators with maximum reachable workspace.

Acknowledgments

The support of grant NSC93 – 2212 - E011-032 from the National Science Council of Taiwan is gratefully acknowledged.

References

1. J. P. Merlet, "Determination of 6D workspaces of Gough-type parallel manipulator and comparison between different geometries", *Int. J. Robot. Res.* **18**(9), 902–916 (1999).
2. E. J. Haug, C. M. Luh, F. A. Adkins and J. Y. Wang, "Numerical algorithms for mapping boundaries of manipulator workspaces", *Trans. ASME J. Mech. Des.* **118**(2), 228–234 (1996).
3. C. M. Luh, F. A. Adkins, E. J. Haug and C. C. Qiu, "Working capability analysis of Stewart platforms", *Trans. ASME J. Mech. Des.* **118**(2), 220–227 (1996).
4. O. Masory and J. Wang, "Workspace evaluation of Stewart platform", *Adv. Robotics* **9**(4), 443–461 ((1995)).
5. I. A. Bonev and J. Ryu, "A new approach to orientation workspace analysis of 6-DOF parallel manipulators", *Mech. and Mach. Theory* **36**(1), 15–28 (2001).
6. M. Z. A. Majid, Z. Huang and Y. L. Yao, "Workspace analysis of a six-degrees of freedom, three-prismatic-prismatic-spheric-revolute parallel manipulator", *Adv. Manuf. Technol.* **16**, 441–449 (2000).